2013

Engineering Geobacter sulferreducens to produce a highly cohesive conductive matrix with enhanced capacity for current production

Ching Leang
Nikhil S. Malvankar
Ashley E. Franks
Kelly P. Nevin
Derek R. Lovley, *University of Massachusetts - Amherst*

Energy & Environmental Science

RSC Publishing

PAPER

View Article Online
View Journal | View Issue

Cite this: *Energy Environ. Sci.*, 2013, **6**, 1901

Engineering *Geobacter sulfurreducens* to produce a highly cohesive conductive matrix with enhanced capacity for current production†

Ching Leang,*[a] Nikhil S. Malvankar,[ab] Ashley E. Franks,‡[a] Kelly P. Nevin[a] and Derek R. Lovley[a]

Received 6th February 2013
Accepted 19th April 2013

DOI: 10.1039/c3ee40441b

www.rsc.org/ees

The conductive biofilms of *Geobacter sulfurreducens* have potential applications in renewable energy, bioremediation, and bioelectronics. In an attempt to alter biofilm properties, genes encoding proteins with a PilZ domain were deleted from the *G. sulfurreducens* genome. A strain, in which the gene GSU1240 was deleted, designated strain CL-1, formed biofilms much more effectively than did the wild-type strain. Increased production of pili and exopolysaccharide were associated with the enhanced biofilm production. When grown with an electrode as the electron acceptor CL-1 produced biofilms that were 6-fold more conductive than wild-type biofilms. The greater conductivity lowered the potential losses in microbial fuel cells, decreasing the charge transfer resistance at the biofilm–anode surface by *ca.* 60% and lowering the formal potential by 50 mV. These lower potential losses increased the potential energy of electrons reaching the biofilm–anode interface and enabled strain CL-1 to produce 70% higher power densities than the wild-type strain. Current-producing biofilms were highly cohesive and could be peeled off graphite electrodes intact, yielding a novel conductive biological material. This study demonstrates that simple genetic manipulation can yield improved bioelectronics materials with energy applications.

Broader context

Long-range electron transport through microbial biofilms has applications for the conversion of organic wastes to methane in anaerobic wastewater digesters or electricity in microbial fuel cells, as well as for microbial electrosynthesis, a process in which microorganisms use electrical energy to produce fuels and other organic commodities from carbon dioxide. *Geobacter sulfurreducens* naturally produces biofilms that are electrically conductive, but genetic engineering offers the possibility of constructing strains that are superior to what natural selection has provided. In this first reported attempt to genetically manipulate *G. sulfurreducens* biofilm formation we describe a strain produced *via* a gene deletion that generates biofilms with enhanced cohesiveness, conductivity, and capacity for current production. These results demonstrate how synthetic biology may significantly contribute to the emerging field of electromicrobiology.

Introduction

Modifying the capacity of microorganisms for extracellular electron exchange may benefit bioenergy applications. Microorganisms with superior capability for current production from organic compounds have been recovered through selective pressure for rapid current production[1,2] and additional increases in current-producing capabilities may be feasible with this approach. An alternative strategy is to genetically engineer organisms for enhanced current production based on an understanding of the physiology of this process.

The importance of direct interspecies electron transfer for the conversion of wastes to methane[3–5] and extracellular electron transfer in groundwater bioremediation[6] suggests that strains with improved capacity for long-range electron transport may have additional applications in bioenergy and bioremediation.

Geobacter sulfurreducens produces the highest current densities of any organism available in pure culture[7] and thus could be considered as a good chassis from which to genetically develop strains with better capacity for current production. A unique feature of *G. sulfurreducens* is its ability to form thick, electrically conductive biofilms.[8–10] Differences in biofilm morphology and electrical properties between strains of *G. sulfurreducens* are associated with substantial differences in

[a]*Department of Microbiology, University of Massachusetts, Amherst, Massachusetts, 01003, USA. E-mail: leang@microbio.umass.edu; Fax: +1-413-577-4660; Tel: +1-413-577-4666*

[b]*Department of Physics, University of Massachusetts, Amherst, Massachusetts, 01003, USA*

† Electronic supplementary information (ESI) available. See DOI: 10.1039/c3ee40441b

‡ Present address: Department of Microbiology, La Trobe University, Melbourne, Victoria, 3086, Australia.

the capacity for current production. For example, the KN400 strain of *G. sulfurreducens*, which produces higher current densities than the DL-1 strain, more readily adheres to surfaces and produces biofilms with less pillar structures than the DL-1 strain. Furthermore, KN400 biofilms are more conductive, which is associated with a higher abundance of electrically conductive pili and a lower outer-surface cytochrome content.[2,8,11]

These results suggest that the appropriate modifications to biofilm structure can have a positive impact on current densities. Levels of bis-(3′–5′)-cyclic dimeric guanosine monophosphate (c-di-GMP) in microbial cells can influence biofilm formation.[12–14] One class of receptors for c-di-GMP are proteins containing PilZ domains. Upon binding to c-di-GMP, activated PilZ domain proteins regulate downstream protein activities at the post-translational level through protein–protein interactions.[12–14] Ten genes encoding proteins containing PilZ domains were identified in the *G. sulfurreducens* genome.[15]

In the study reported here, the impact of deleting genes for proteins with PilZ domains on biofilm formation and current production was evaluated. Deletion of one of these genes yielded a strain with a highly cohesive biofilm that was more conductive and produced higher current densities than the wild-type strain, demonstrating the potential to tune the electrical properties of living, self-renewing materials with genetic engineering.

Results and discussion

Identification of a regulatory protein involved in biofilm formation in *G. sulfurreducens*

Of the ten genes that were predicted to encode PilZ domain proteins, five genes, GSU3263, GSU0877, GSU1192, GSU3033 and GSU1240 are well conserved among the completed *Geobacter* genomes of *G. metallireducens*,[16] *G. uraniireducens*, *G. bemidjiensis*[17] and *G. sulfurreducens*.[18] Attempts to delete the genes for these five conserved PilZ domain proteins only yielded viable strains in which either the gene GSU1240 or GSU3263 was deleted. The GSU1240-deficient mutant, designated strain CL-1, was chosen for further studies because this strain readily produced aggregates when grown with fumarate as the electron acceptor, a condition in which wild-type cells do not aggregate.

Strain CL-1 grew at a similar growth rate as the wild-type in medium with acetate as the electron donor and fumarate as the electron acceptor (ESI, Fig. 1†). However, the CL-1 culture had a different appearance, forming aggregates, and biofilms which stuck to the side and the bottom of culture tubes (Fig. 1a). In glass attachment assays 8-fold more CL-1 biomass attached than the wild-type (Fig. 1b).

Strain CL-1 produced more pili than the wild-type strain (Fig. 2). The multi-heme *c*-type cytochrome, OmcS, is specifically associated with pili in wild-type cells.[19] Heme-staining revealed a higher abundance of cytochrome with a molecular weight consistent with OmcS in CL-1 (Fig. 3a) and Western blot analysis with OmcS-specific antiserum confirmed higher production of OmcS in CL-1 (Fig. 3a). Immunogold labeling coupled with transmission electron microscopy demonstrated that OmcS was localized on the pili of CL-1 (Fig. 3b), as previously reported for wild-type.[19]

When cells grown in medium containing acetate as the electron donor and fumarate as the electron acceptor (NBAF) were stained with ruthenium red, an abundant exopolysaccharide matrix surrounding the cells was apparent with strain CL-1 (Fig. 4a) that was not present in wild-type (Fig. 4b). Minimal extracellular matrix was apparent for both the wild-type and CL-1 strains when ruthenium red were omitted (ESI,

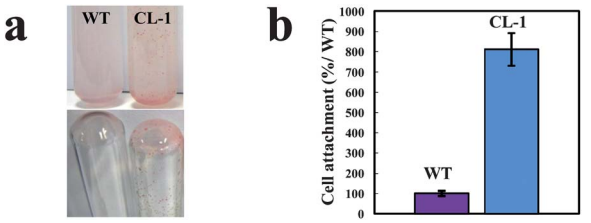

Fig. 1 Enhanced biofilm formation of strain CL-1. (a) Increased aggregate and biofilm formation of strain CL-1 in acetate–fumarate medium (NBAF) (upper panel) and attachment of aggregates to the glass in inverted culture tubes (lower panel). (b) Increased attachment of CL-1 biomass to glass surface of culture tubes as quantified with crystal violet stain. Data are means ± standard deviations of triplicates.

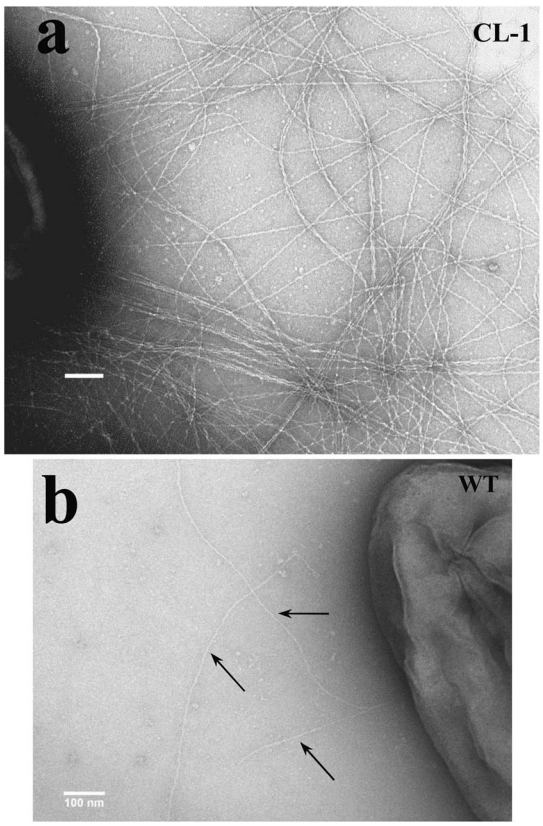

Fig. 2 Transmission electron micrographs of negatively stained cells demonstrating enhanced pili formation of strain CL-1 (a) *versus* wild-type (b) in cells grown in acetate–fumarate medium (NBAF) at 25 °C to induce pili production. Scale bar represents 100 nm. Images were representatives of 100 cells observed from either wild-type or CL-1 strains.

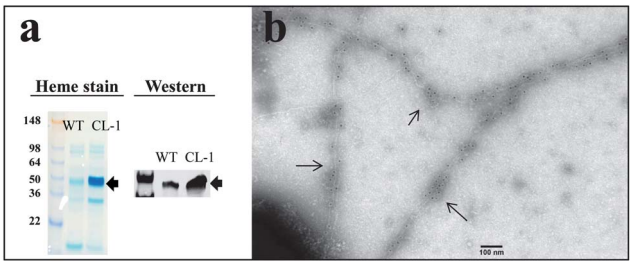

Fig. 3 OmcS abundance and localization. (a) Heme stain of SDS-PAGE (left panel) showing increased abundance in CL-1 of a heme-containing protein migrating at *ca.* 50 kDa molecular weight expected for OmcS and Western blot analysis (right panel) confirming that the heme-containing protein is OmcS. (b) Transmission electron micrograph of negatively stained CL-1, which was labelled first with anti-OmcS rabbit polyclonal antibodies and then with anti-rabbit secondary antibody conjugated with 10 nm-gold. OmcS was specifically associated with pili. Images are representative of fifteen images taken from the CL-1 strain.

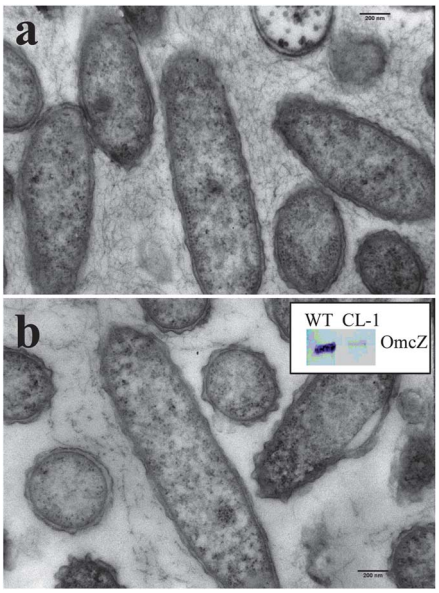

Fig. 4 Transmission electron micrographs of thin sections stained with ruthenium red demonstrating extensive exopolysaccharide web in CL-1 (a), but not wild-type (b). Two biological samples of both strains were prepared and stained with ruthenium red. Images were representatives of 10 images taken from either wild-type or CL-1 strains. Western blot analysis with anti-OmcZ antibody (b, inset).

Fig. 2†). OmcZ, an outer-surface multi-heme *c*-type cytochrome[20,21] potentially associated with exopolysaccharide,[22] was less abundant in CL-1 cultures compared to wild-type (Fig. 4b inset).

Biofilm on positively poised anodes

When grown with a positively poised (+300 mV *versus* Ag/AgCl) graphite anode strain CL-1 produced more current (*ca.* 16–18 mA) than the wild-type (*ca.* 12–14 mA).[10,23] Scanning electron microscopy revealed that the wild-type strain produced a biofilm with mushroom-shaped structures (Fig. 5a), as previously reported,[10,24] whereas the CL-1 biofilm was homogenous and

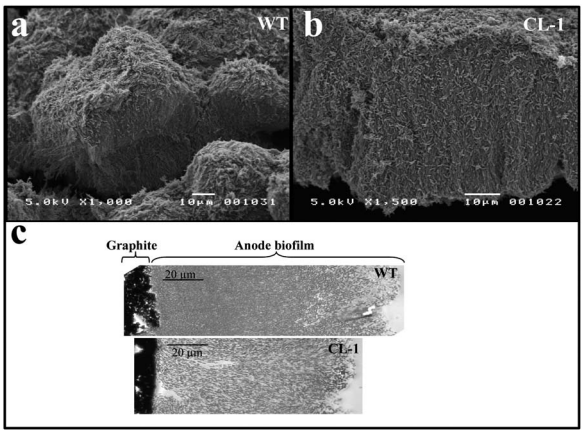

Fig. 5 Biofilms growing on poised graphite anodes. Scanning electron micrographs of wild-type (a) and CL-1 (b) strains. Two biological samples of either wild-type or the CL-1 strain were prepared for scanning electron micrograph. Images were representatives of 10 images taken from the wild-type or CL-1 strains. (c) Light microscope images of thin sectioned anode biofilm cells stained with toluidine blue.

flat (Fig. 5b). Examination with light microscopy of semi-thin sections (200 μm) of anode biofilms embedded in acrylic resin demonstrated that the wild-type produced a thicker biofilm (*ca.* 120–160 μm) than CL-1 (*ca.* 90 μm) (Fig. 5c). The CL-1 biofilm was highly cohesive and could be pulled off the anode intact (Fig. 6). The wild-type biofilm lacked this high degree of cohesiveness.

Immunogold labeling of anode biofilm thin-sections revealed that OmcS was distributed throughout the biofilms of both wild-type (Fig. 7a and b) and CL-1 (Fig. 7c and d), but in higher abundance in the CL-1 biofilms. OmcZ was scarce in CL-1 anode biofilms (Fig. 8), and near the anode–biofilm interface where OmcZ was previously observed to accumulate in wild-type biofilms.[20] Previous studies suggested that OmcZ was necessary in order to produce high current densities with wild-type cells,[23,25] but the low abundance of OmcZ as well as the lack

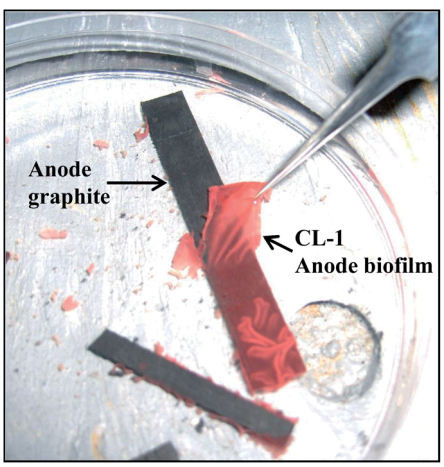

Fig. 6 Cohesive nature of CL-1 anode biofilms. This was observed consistently with all CL-1 current-producing anode biofilms.

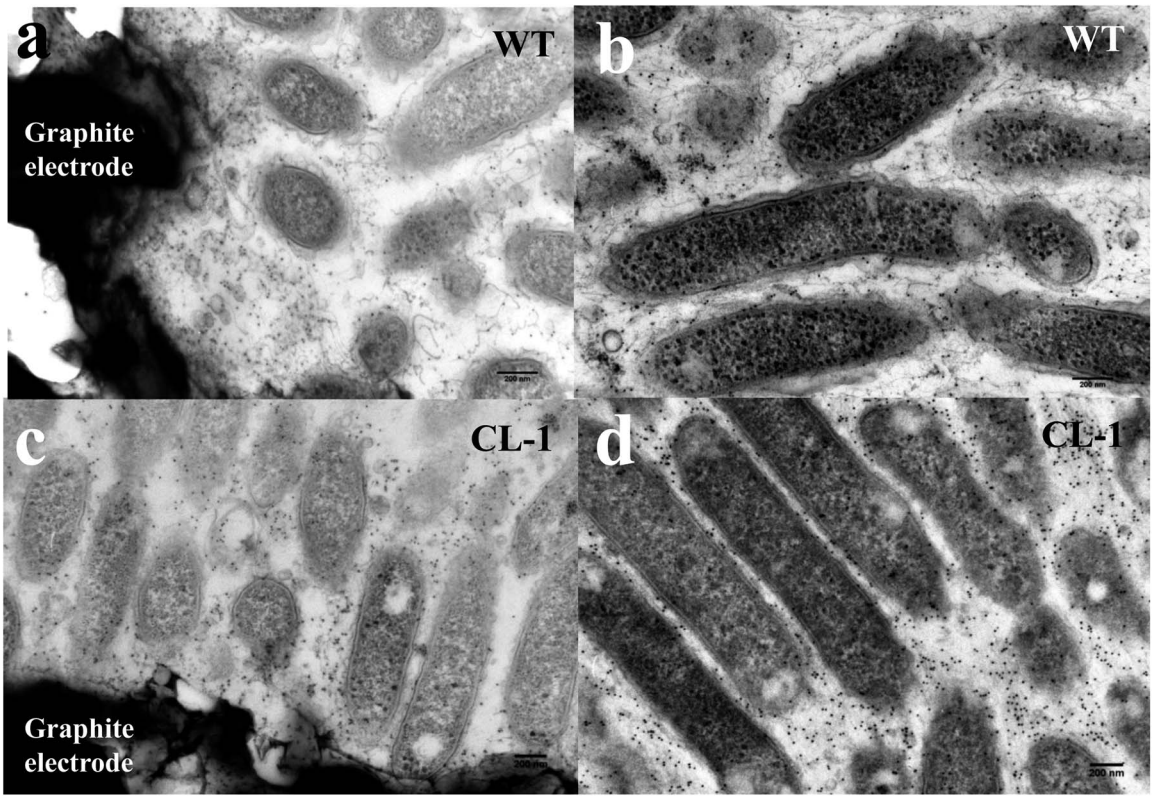

Fig. 7 Transmission electron micrographs of immunogold-labeled anti-OmcS thin sections of the wild-type (a and b) and the CL-1 strain (c and d) current producing anode biofilms demonstrating distribution of OmcS throughout both biofilms. Images are representatives of 100 images taken from either the wild-type or the CL-1 strain.

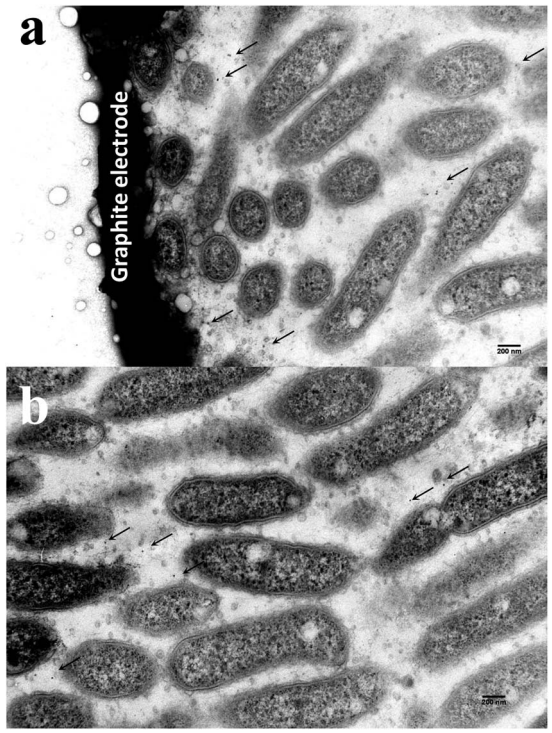

Fig. 8 Transmission electron micrographs of immunogold-labeled anti-OmcZ thin sections of the CL-1 anode biofilms near the anode surface (a) and in the bulk biofilm (b). Arrows point to scarce OmcZ labeling with no apparent accumulation of OmcZ at the anode–biofilm interface previously reported for wild-type. Images are representatives of 100 images taken for the CL-1 strain.

of OmcZ accumulation at the anode surface in the CL-1 biofilms suggested that OmcZ was not as important in this strain.

Anode biofilm properties in fuel cell mode

Controlling anode potential with a potentiostat makes it possible to maintain controlled conditions for strain comparisons, but for the practical goal of producing current, studies with unpoised anodes in a microbial fuel cell are more relevant. Under these "true fuel cell" and not-cathode-limiting conditions,[2,11] strain CL-1 produced a maximum current density that was 50% higher than that of the wild-type and the maximum power density of CL-1 was 70% higher than the wild-type (Fig. 9a).

Current densities have previously been correlated with biofilm conductivity.[26] Strain CL-1 produced an anode biofilm that was six times more conductive than the wild-type (Fig. 9b). The higher conductivity of the CL-1 biofilms was associated with a higher abundance of PilA (Fig. 9b inset), the structural protein for the conductive pili of *G. sulfurreducens*.[27] This finding is consistent with previous studies, which have demonstrated a direct correspondence between the abundance of PilA and the biofilm conductivity of different gene-deletion strains of *G. sulfurreducens*.[8]

Increases in biofilm conductivity have previously been associated with decreases in charge transfer resistance at the anode–biofilm interface,[26] which can be attributed to lower potential losses during electron transport through the

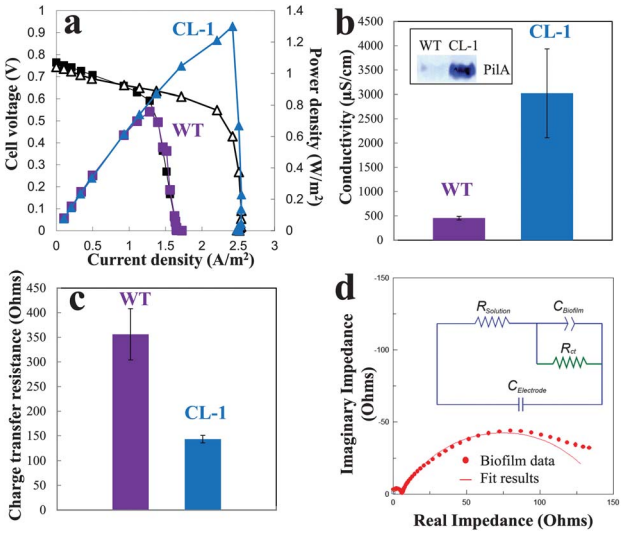

Fig. 9 Electrical and electrochemical characteristics of the anode biofilms of wild-type and strain CL-1 grown in ministack microbial fuel cell. (a) Current–voltage and current–power density relationships. Power densities: WT, purple squares; CL-1, blue triangles; polarization curves: WT, black squares; CL-1, black triangles. (b) Biofilm conductivity with inset showing Western blot analysis of PilA expression. (c) Biofilm charge transfer resistance. (d) CL-1 biofilm impedance spectra with inset showing the equivalent circuit used to extract the fitting parameters. $R_{Solution}$: electrolyte resistance. $C_{Biofilm}$: biofilm capacitance, R_{ct}: charge transfer resistance, $C_{Electrode}$: geometrical capacitance due to electrodes. Results are representative of duplicate biofilms. Data are means ± standard deviations of three measurements.

biofilm.[26,28] The charge transfer resistance was extracted by fitting the equivalent circuit model shown in Fig. 9d (inset) to the impedance spectrum (Fig. 9d) as described previously.[26,28] The charge transfer resistance of the CL-1 biofilm was only 40% that of the wild-type (Fig. 9c). It has previously been demonstrated that the decrease in charge transfer resistance of the anode biofilms lowers the potential losses in the microbial fuel cell, thus enhancing the power production.[26,28] The decrease in potential losses in CL-1 biofilms was also apparent in cyclic voltammetry studies which revealed that the formal potential decreased from −350 mV (*versus* Ag/AgCl) for the wild-type strain to −400 mV for strain CL-1 (Fig. 10). This is the expected result with higher biofilm conductivity because electrons are delivered to the anode with increased energy, thus causing lower potential losses.[25,26,28]

Materials and methods

Bacterial strains and culturing conditions

Geobacter sulfurreducens strains were routinely cultured as previously described,[29] under anaerobic conditions, at 30 °C, in the medium designated NBAF[29] in which acetate serves as the electron donor and fumarate is the electron acceptor. *G. sulfurreducens* wild-type strain DL-1 (ref. 30) and the OmcS deletion mutant[31] were obtained from our laboratory culture collection.

Cells were grown with a poised graphite electrode as the electron acceptor in a two-chambered H-cell system as previously described.[23,32] For thin sectioning (60–80 nm) of the

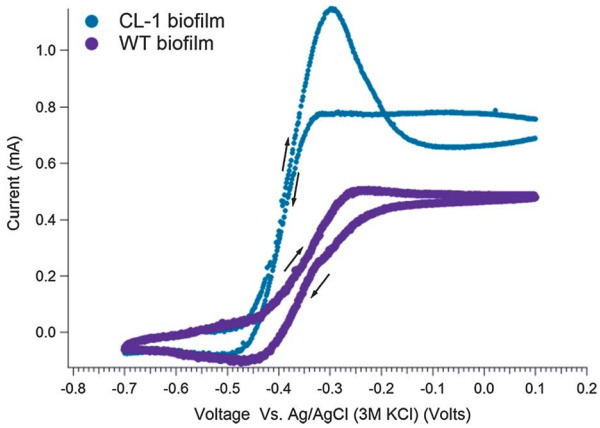

Fig. 10 Cyclic voltammetry of CL-1 and wild-type anode biofilm in the presence of 10 mM acetate. Arrows indicate the direction of cathodic and anodic scan. The cathodic scan corresponds to the lower current curve whereas the anodic scan corresponds to the upper current curve. Scan rate is 10 mV s^{-1}. Results are representative of duplicate biofilms.

anode-grown biofilm, the stick graphite was replaced with polished "fingered" graphite as previously described.[24]

Single gene replacement

Sequences were deleted with single-step gene replacement as previously described.[33] To disrupt the GSU1240 gene, a 1.56 kb linear DNA fragment was generated by recombinant PCR[33,34] from three primary PCR products: (1) the 5′ end of GSU1240 (0.36 kb, amplified with primers GSU1240KO-01 (5′-GCAGACTACGAG GAACTG-3′) and GSU1240KO-02 (5′-CCGTGCTCTTCGACGATG-3′)); (2) 3′ end of the GSU1240 gene (0.32 kb, amplified with primers GSU1240KO-05 (5′-GGAACGTGAGCGTTACCG-3′) and GSU1240KO-06 (5′-CGATGTTCAGGAAGTGTG-3′)); and (3) a chloramphenicol resistant cassette (Cm^R) (0.88 kb, amplified with primers GSU1240KO-03 (5′-CATCGTCGAAGAGCACGGACGGAAGATCACT TCGC-3′) and GSU1240KO-04 (5′-CGGTAACGCTCACGTTC CAGGGCACCAATAACTGCC-3′)). Recombinant PCR was performed with these three PCR products as templates with distal primer pairs, GSU1240KO-01/GSU1240KO-06. PCR conditions were as previously described, except that the annealing temperature was 58 °C.[33]

Electroporation, mutant isolation and genotype confirmation were performed as previously described.[29,33] One of the colonies with correct genotype was chosen as the representative strain for further studies and was designated strain CL-1.

Electron microscopy and immunogold labeling

For observing cell appendages of whole cells, cultures (20 μl) were placed on a 400-mesh carbon-coated copper grids for 1–5 minutes, then stained with 2% uranyl acetate and observed with a JEOL 100S transmission electron microscope operated at 80 kV.

For observation of the localizations of OmcS and OmcZ within the current-producing anode biofilms, the anode biofilm cells which were still attached to the graphite were cut into small pieces (0.5 cm × 1 cm) and were fixed and embedded in LR White (medium grade, EMS). Briefly, cells were fixed with

freshly made fixative (2% paraformaldehyde and 0.5% glutaraldehyde in 50 mM PIPES pH 7.2) for one hour at room temperature, washed with 50 mM PIPES for 3 times. Biofilm samples were dehydrated by graded ethanol series (30, 50, 70, 80, 100%; 30 min each stage with gentle agitation) after fixation. The dehydrated samples were infiltrated with LR White and polymerized using a UV light (2 × 4 W BLB, 405 nm) or polymerized at 55 °C for overnight. Thin sections (60–80 nm) of embedded anode biofilms were made with a microtome (ULtracut S, Leica, Microsystems, Germany) and were mounted on colloidion-coated gold-gilded copper grids. Sections were either positively stained with 2% uranyl acetate or immunogold labeled before staining with uranyl acetate, and were observed with a JEOL 100S transmission electron microscope at 80 kV. Images were taken digitally with MaxIm-DL software and analyzed with ImageJ (http://rsbweb.nih.gov/ij/index.html).

Immunogold labeling protocol was adapted from Durand *et al.*[35] Briefly, the sections were treated with 3% bovine serum albumin (BSA) in PBS for 15 minutes, and then labeled for an hour at room temperature with previously described OmcS or OmcZ antiserum.[19–21] After three washes in PBS buffer, the sections were incubated for 1 hour with 10 nm gold-labeled goat anti-rabbit IgG (Sigma) in PBS with 0.3% BSA. The sections were washed 3 times in PBS (3 minutes each) and once briefly in Milli-Q water, stained with 2% uranyl acetate, and examined with the transmission electron microscope as described above.

For observing exopolysaccharides, NBAF grown cells were double fixed, dehydrated then embedded in LR White as described in Etienne *et al.*[36] Briefly, cells were fixed in freshly made fixative (2% paraformaldehyde, 0.5% glutaraldehyde and 0.05% (w/v) ruthenium red in 0.1 M, pH 7.2 cacodylate buffer) for 1 hour at room temperature. Cells were washed three times in cacodylate buffer (0.1 M, pH 7.2), postfixed for one hour in 1% osmium tetroxide and 0.05% ruthenium red, and then washed three times in cacodylate buffer.[36] Cells were dehydrated and embedded in LR White as described above. Thin sections (60–80 nm) were cut with a microtome as described above and sections were stained with 2% uranyl acetate and observed with the transmission electron microscope.

Cell attachment assays

Mid-log cells were inoculated into fresh medium and incubated for 3 days. Planktonic cells were decanted and the culture tubes were washed twice in Milli-Q water. Remaining cells that were attached to tubes were stained with 0.1% crystal violet solution (10 ml) for 5 min and washed twice in Milli-Q water. Crystal violet stain was solubilized in ethanol (10 ml) overnight and was measured at 580 nm in a Genesys 2 spectrophotometer (Spectronic Instruments).

Current and power production in fuel cells

Current and power production was evaluated in the "ministack" microbial fuel cell system.[7] The anode was a small size graphite rod (7.1×10^{-6} m^2 surface area) and the cathode was graphite cloth (2.54 cm × 2.54 cm). Fuel cell voltage was measured across the resistor (560 Ω) and current-density–power relationships were determined as described previously.[2]

Biofilm conductivity measurements

Both wild-type and strain CL-1 were grown on an anode array in which four-gold anodes were each separated by a 50 μm non-conducting gap, as described previously[8] in a "ministack" microbial fuel cell with gold electrodes serving as anode and a carbon cloth as a cathode, connected by a 560 ohms resistor. Once the biofilm bridged the gaps (ESI, Fig. 3†), the biofilm conductivity was measured with the 4-probe approach as described previously.[8,26] A source meter (Keithley 2400) was used to apply a fixed current between outer two of the four electrodes and to measure the potential drop between two inner electrodes,[36] by measuring the voltage for each current every second over a period of 100 seconds, after reaching the steady-state. An additional high-impedance voltmeter (Keithley 2000) was used to record the output voltage of the current source to measure conductance.[36] As previously described,[8] conformal mapping (the Schwarz–Christoffel transformation) was employed to calculate biofilm conductivity (σ) from measured conductance (G) according to following formula

$$\sigma = G\frac{\pi}{L}\Big/\ln\left(\frac{8g}{\pi a}\right)$$

where L is the length of the electrodes ($L = 2.54$ cm); a is the half-spacing between the electrodes ($2a = 50$ μm) and g is the biofilm thickness. This formula is valid for the limiting case $a < g \ll b$ where b is the half width of the electrodes ($2b = 2.54$ cm).

Charge transfer resistance and cyclic voltammetry measurements

All electrochemical experiments were performed using Solartron 1287 potentiostat/galvanostat at room temperature. Impedance spectroscopy was performed using a Solartron 1252/1287 impedance analyzer. To measure impedance spectra and cyclic voltammetry (CV) of anode biofilms, gold electrodes serving as anode, were externally short circuited and an impedance spectrum and CV of the biofilm was measured using the 3-electrode cell with anode as the working electrode and the cathode comprised of the carbon cloth as the counter electrode. Electrochemical impedance spectroscopy (EIS) was employed to measure charge transfer resistance of anode biofilm as described previously.[26,28] EIS measurements were carried out in a frequency range of 300 kHz to 100 mHz with an ac signal of 0.1 V amplitude. For all impedance measurements, open circuit potential was monitored until it reached a constant value before over imposing an ac signal. All comparisons were made with the charge transfer resistance and biofilm resistance values measured at open circuit potential. Charge transfer resistance values were extracted by fitting to the impedance spectrum (Fig. 9d) an equivalent circuit in which solution resistance is in series with parallel combination of capacitance and charge transfer resistance (Fig. 9d inset). Data fitting was performed with ZView software (Scribner Inc.) which uses LEVM algorithm developed by J. Ross Macdonald. Cyclic voltammetry was

performed in the voltage range −0.7 V to 0.1 V *vs.* Ag/AgCl (3 M KCl) reference electrode at scan rate 10 mV s^{-1}. The anodic scan (−0.7 V to 0.1 V) was performed first, shown as a forward arrow, followed by the cathodic scan, shown as a reverse arrow (Fig. 10). The cathodic scan corresponds to the lower current curve in Fig. 10 whereas the anodic scan corresponds to the upper current curve in Fig. 10. The CV experiments were initiated after a stable open circuit potential was observed for the anode. The CV data was collected using CoreView software (Scribner Inc.) and analyzed using IGOR Pro (Wavemetrics Inc.).

Analytical techniques

Protein concentration was determined using the bicinchoninic acid method with bovine serum albumin as a standard.[37] Western blot analyses and immunoreactive band visualizations were carried out by using appropriate antiserums with One-Step Western Complete Kit with TMB (GenScript) according to the manufacturer's instruction. Growth of cultures with fumarate as the electron acceptor was monitored by measuring turbidity at 600 nm in a Genesys 2 spectrophotometer (Spectronic Instruments).

Conclusions

The results demonstrate that the deletion of a single gene in *G. sulfurreducens* can have a significant impact on its capacity for current production. The CL-1 strain had multiple phenotypic differences from the wild-type DL-1 strain from which it was constructed, presumably because the deleted gene is part of regulatory circuit that impacts the expression of many genes. Important differences between the CL-1 and wild-type strains were greater production of pili and pili-associated OmcS in CL-1, but less production of OmcZ. A positive association between higher pili abundance and improved biofilm conductivity and current production has been observed in studies in which genes for multiple outer-surface *c*-type cytochromes were deleted.[26] Furthermore, the KN400 strain of *G. sulfurreducens*, which produces more current and has higher biofilm conductivities than the wild-type strain DL-1 also has a higher abundance of pili.[2] OmcS is not required for current production in the bioelectrical systems used for evaluation of current production in this study.[8,38] OmcZ, which is required for high-density current production in the wild-type strain,[38] was in much lower abundance in the CL-1 strain. The specific localization of OmcZ at the anode–biofilm interface and the poor ability of an OmcZ-deficient strain to exchange electrons with graphite electrodes,[25] have led to the suggestion that the role of OmcZ is to facilitate electron transfer from the biofilm to the anode.[20] The ability of the CL-1 biofilms to provide electrons to the anode at a substantially lower potential may alleviate the need for abundant OmcZ to facilitate this electron transfer. Evaluation of this hypothesis will require the construction of additional mutant strains that are beyond the scope of this study.

The high cohesiveness of the CL-1 biofilms, is an unexpected phenotype, which offers the possibility of producing sheets of a biological material with conductivities comparable to that of synthetic conducting polymeric films such as nanostructured polyaniline and polyacetylene.[8] These properties coupled with the ability of *G. sulfurreducens* biofilms to function as living supercapacitors[39] and transistors,[8] suggest that there may be bioelectronics applications for *G. sulfurreducens* beyond converting organic substrates to electricity.

Acknowledgements

We thank Dale Callaham for his guidance in electron microscopy works and helpful discussions. We are grateful for the excellent technical support from Manju Sharma, Trevor L. Woodard and Joy Ward. This research was supported by the Office of Naval Research (grant no. N00014-10-1-0084 and N00014-12-1-0229).

Notes and references

1 Y. Liu, F. Harnisch, K. Fricke, R. Sietmann and U. Schroder, *Biosens. Bioelectron.*, 2008, **24**, 1012–1017.
2 H. Yi, K. P. Nevin, B. C. Kim, A. E. Franks, A. Klimes, L. M. Tender and D. R. Lovley, *Biosens. Bioelectron.*, 2009, **24**, 3498–3503.
3 F. Liu, A.-E. Rotaru, P. M. Shrestha, N. S. Malvankar, K. P. Nevin and D. R. Lovley, *Energy Environ. Sci.*, 2012, **5**, 8982–8989.
4 D. R. Lovley, *Energy Environ. Sci.*, 2011, **4**, 4896–4906.
5 M. Morita, N. S. Malvankar, A. E. Franks, Z. M. Summers, L. Giloteaux, A. E. Rotaru, C. Rotaru and D. R. Lovley, *mBio*, 2011, **2**, e00159-11, DOI: 10.1128/mBio.00159-11.
6 D. R. Lovley, T. Ueki, T. Zhang, N. S. Malvankar, P. M. Shrestha, K. A. Flanagan, M. Aklujkar, J. E. Butler, L. Giloteaux, A. E. Rotaru, D. E. Holmes, A. E. Franks, R. Orellana, C. Risso and K. P. Nevin, *Adv. Microb. Physiol.*, 2011, **59**, 1–100.
7 K. P. Nevin, H. Richter, S. F. Covalla, J. P. Johnson, T. L. Woodard, A. L. Orloff, H. Jia, M. Zhang and D. R. Lovley, *Environ. Microbiol.*, 2008, **10**, 2505–2514.
8 N. S. Malvankar, M. Vargas, K. P. Nevin, A. E. Franks, C. Leang, B.-C. Kim, K. Inoue, T. Mester, S. F. Covalla, J. P. Johnson, V. M. Rotello, M. T. Tuominen and D. R. Lovley, *Nat. Nanotechnol.*, 2011, **6**, 573–579.
9 N. S. Malvankar and D. R. Lovley, *ChemSusChem*, 2012, **5**, 1039–1046.
10 G. Reguera, K. P. Nevin, J. S. Nicoll, S. F. Covalla, T. L. Woodard and D. R. Lovley, *Appl. Environ. Microbiol.*, 2006, **72**, 7345–7348.
11 N. S. Malvankar, M. T. Tuominen and D. R. Lovley, *Energy Environ. Sci.*, 2012, **5**, 8651–8659.
12 H. Sondermann, N. J. Shikuma and F. H. Yildiz, *Curr. Opin. Microbiol.*, 2012, **15**, 140–146.
13 C. D. Boyd and G. A. O'Toole, *Annu. Rev. Cell Dev. Biol.*, 2012, **28**, 439–462.
14 U. Romling, M. Y. Galperin and M. Gomelsky, *Microbiol. Mol. Biol. Rev.*, 2013, **77**, 1–52.
15 D. Amikam and M. Y. Galperin, *Bioinformatics*, 2006, **22**, 3–6.

16 M. Aklujkar, J. Krushkal, G. DiBartolo, A. Lapidus, M. L. Land and D. R. Lovley, *BMC Microbiol.*, 2009, **9**, 109.
17 M. Aklujkar, N. Young, D. Holmes, M. Chavan, C. Risso, H. Kiss, C. Han, M. Land and D. Lovley, *BMC Genomics*, 2010, **11**, 490.
18 B. A. Methé, K. E. Nelson, J. A. Eisen, I. T. Paulsen, W. Nelson, J. F. Heidelberg, D. Wu, M. Wu, N. Ward, M. J. Beanan, R. J. Dodson, R. Madupu, L. M. Brinkac, S. C. Daugherty, R. T. DeBoy, A. S. Durkin, M. Gwinn, J. F. Kolonay, S. A. Sullivan, D. H. Haft, J. Selengut, T. M. Davidsen, N. Zafar, O. White, B. Tran, C. Romero, H. A. Forberger, J. Weidman, H. Khouri, T. V. Feldblyum, T. R. Utterback, S. E. Van Aken, D. R. Lovley and C. M. Fraser, *Science*, 2003, **302**, 1967–1969.
19 C. Leang, X. Qian, T. Mester and D. R. Lovley, *Appl. Environ. Microbiol.*, 2010, **76**, 4080–4084.
20 K. Inoue, C. Leang, A. E. Franks, T. L. Woodard, K. P. Nevin and D. R. Lovley, *Environ. Microbiol. Rep.*, 2010, **3**, 211–217.
21 K. Inoue, X. Qian, L. Morgado, B. C. Kim, T. Mester, M. Izallalen, C. A. Salgueiro and D. R. Lovley, *Appl. Environ. Microbiol.*, 2010, **76**, 3999–4007.
22 J. B. Rollefson, C. S. Stephen, M. Tien and D. R. Bond, *J. Bacteriol.*, 2011, **193**, 1023–1033.
23 K. P. Nevin, B. C. Kim, R. H. Glaven, J. P. Johnson, T. L. Woodard, B. A. Methe, R. J. Didonato, S. F. Covalla, A. E. Franks, A. Liu and D. R. Lovley, *PLoS One*, 2009, **4**, e5628.
24 A. E. Franks, K. P. Nevin, R. H. Glaven and D. R. Lovley, *ISME J.*, 2010, **4**, 509–519.
25 H. Richter, K. P. Nevin, H. F. Jia, D. A. Lowy, D. R. Lovley and L. M. Tender, *Energy Environ. Sci.*, 2009, **2**, 506–516.
26 N. S. Malvankar, M. T. Tuominen and D. R. Lovley, *Energy Environ. Sci.*, 2012, **5**, 5790–5797.
27 G. Reguera, K. D. McCarthy, T. Mehta, J. S. Nicoll, M. T. Tuominen and D. R. Lovley, *Nature*, 2005, **435**, 1098–1101.
28 N. S. Malvankar, J. Lau, K. P. Nevin, A. E. Franks, M. T. Tuominen and D. R. Lovley, *Appl. Environ. Microbiol.*, 2012, **78**, 5967–5971.
29 M. V. Coppi, C. Leang, S. J. Sandler and D. R. Lovley, *Appl. Environ. Microbiol.*, 2001, **67**, 3180–3187.
30 F. Caccavo, Jr, D. J. Lonergan, D. R. Lovley, M. Davis, J. F. Stolz and M. J. McInerney, *Appl. Environ. Microbiol.*, 1994, **60**, 3752–3759.
31 T. Mehta, M. V. Coppi, S. E. Childers and D. R. Lovley, *Appl. Environ. Microbiol.*, 2005, **71**, 8634–8641.
32 D. R. Bond and D. R. Lovley, *Appl. Environ. Microbiol.*, 2003, **69**, 1548–1555.
33 J. R. Lloyd, C. Leang, A. L. H. Myerson, M. V. Coppi, S. Cuifo, B. Methe, S. J. Sandler and D. R. Lovley, *Biochem. J.*, 2003, **369**, 153–161.
34 K. C. Murphy, K. G. Campellone and A. R. Poteete, *Gene*, 2000, **246**, 321–330.
35 E. Durand, A. Bernadac, G. Ball, A. Lazdunski, J. N. Sturgis and A. Filloux, *J. Bacteriol.*, 2003, **185**, 2749–2758.
36 G. Etienne, C. Villeneuve, H. Billman-Jacobe, C. Astarie-Dequeker, M. A. Dupont and M. Daffe, *Microbiology*, 2002, **148**, 3089–3100.
37 P. K. Smith, R. I. Krohn, G. T. Hermanson, A. K. Mallia, F. H. Gartner, M. D. Provenzano, E. K. Fujimoto, N. M. Goeke, B. J. Olson and D. C. Klenk, *Anal. Biochem.*, 1985, **150**, 76–85.
38 K. Nevin, B. Kim, R. Glaven, J. Johnson, T. Woodard, B. Methe, R. DiDonato, S. Covalla, A. Franks and A. Liu, *PLoS One*, 2009, **4**, e5628.
39 N. S. Malvankar, T. Mester, M. T. Tuominen and D. R. Lovley, *ChemPhysChem*, 2012, **13**, 463–468.

